ISSN: 2716-9227 Algerian Journal of Engineering and Technology 03 (2020) 028–037 e-ISSN: 2716-9278

Algerian Journal of Engineering and Technology

Journal homepage: https://jetjournal.org/index.php/ajet

Original Article

Corrosion inhibition potentials of *Strichnos spinosa* L. on Aluminium in 0.9M HCl medium: experimental and theoretical investigations

Abdullahi Muhammad Ayuba* and Ameenullah Abdullateef

Department of Pure and Industrial Chemistry, Bayero Universit, Kano, Nigeria

ARTICLE INFO

Article history:
Received 17 September 2020
Revised 11 November 2020
Accepted 21 November 2020

Keywords:
Corrosion inhibition;
Strichnos spinosa L;
Aluminium;
Experimental;
Theoretical.

ABSTRACT

Aluminium is known as one of the most useful metals on earth which is also subject to corrosion under certain environments. Many methods have been used to minimize its corrosion, but the use of inhibitors is widely accepted. The use of green inhibitors has gained wide usage because of its environmental friendliness. The experimental studies of the corrosion inhibition potentials of *Strichnos spinosa* L was carried out using weight-loss and Fourier transform infrared spectroscopy (FTIR), whereas theoretically, quantum chemical parameters and molecular dynamic stimulations of some compounds isolated from the plant in literature were studied. The analyses of the experimental results showed that the extract of *Strichnos spinosa* L. extract decreased the corrosion rate of Aluminium in 0.9M HCl in the order: 0.2g/l < 0.4g/l < 0.6g/l respectively from 303-323K. The inhibition efficiency decreased with increase in temperature and was found to be 84.7%. FTIR results showed that the inhibition mechanism is physical through the functional groups present in the extract. The data obtained were fitted into various adsorption isotherms and relatively the Freundlich isotherm was found to be the best fit. Relying on quantum chemical parameters and molecular dynamic stimulations results, the adsorption/binding strength of the concerned inhibitor molecules on Aluminium surface follows the order Ursolic acid>Betulinic acid>Erythrodiol. The computed adsorption/binding energy values (E_{ads}) for the various isolated compounds from the plant indicate the adsorption process to be non-covalent (physiosorption) which is in good agreement with the experimentally determined adsorption mechanism.

1. Introduction

Corrosion of Aluminium (Al) due to chemical attack by acidic environment is one of the universal problems with financial implications which necessitate protection of Aluminium in many industries including chemical, oil and gas transportation, construction industries among others [1]. Corrosion may be caused by chemical cleaning, pickling and rescaling of the metals in industries [2]. As a result of chemical attack, prevention of Al against corrosion in acid atmosphere is required. The use of chemical inhibitors is one of the most successful methods to avoid deterioration of Al metal. Inhibitors are substances which when employed suppress and reduced the rate of attack of corrosive ions present in the solution which is in contact with the Al surfaces. The use of organic molecules consisting of heteroatoms with unsaturated bonds and/or polar atoms such as S, N, O, P etc. due to the lone pair of electrons present on them adsorbed on to the metal surface, and therefore loss of electrons from the metal surface can be avoided. Thus corrosion inhibition takes place by adsorption of inhibitor molecules on metal surface by providing a protective film which results in corrosion control [3]. In order to overcome the challenges by toxic inhibitors, there is need to focus on research of the use of commercially cheap, non-hazardous and ecological corrosion inhibitors. This biologically mediated innovative type of corrosion inhibitors can be sourced from the available plant sources. Extracts of plant sources are considered as an extremely wealthy source of various chemical compounds like alkaloids, flavonoids, phenolic e.t.c compounds that can be derived by easy methods [4].

* *Corresponding author.*Tel.: +2348062771500
E-mail address: ayubaabdullahi@buk.edu.ng
Peer review under responsibility of University of Echahid Hamma Lakhdar.
http://dx.doi.org/10.5281/zenodo.4402204

A number of such natural products have been investigated for the corrosion inhibition of metals through experimental and theoretical approaches [5-11].

From the findings of the authors in literature, the plant *Strichnos spinosa* L. have not been used to inhibit Al corrosion in HCl solution. The present study attempt to experimentally explore the possibility of using *Strichnos spinosa* L. plant extract for the corrosion inhibition of Aluminium in 0.9M HCl solution at different temperatures. Weight loss method will be employed to evaluate corrosion rate, surface coverage and inhibition efficiencies of the inhibitor. Also, theoretically, evaluation of corrosion inhibition potentials of some isolated compounds from *Strichnos spinosa* L. leaves obtained from literature [12] through assessment of their quantum chemical parameters and molecular dynamic simulations on Aluminium metal surface will be conducted.

2. Materials and Methods

All reagents used for the study were of analar grade and double distilled water was used for all the solution preparations (both stock and working). The concentration of HCl used for the weight loss studies was 0.9M HCl.

2.1 Preparation of Aluminium samples

Aluminium sheet samples of composition (wt %: Al_2O_3 = 99.36, SiO_2 = 0.27, Fe_2O_3 = 0.20, SO_3 = 0.04, K_2O = 0.03 and Cl = 0.03) obtained through energy-dispersive x-ray fluorescence technique were used for the experimental. This material was mechanically press-cut into different coupons, each of dimensions 3 x 2 x 0.12cm. The coupons were wet polished with different grades of SiC abrasive paper (#400 to #1200), degreased by washing with ethanol, cleaned with acetone and allowed to dry in the air before preservation in a desiccator.

2.2 Collection, preparation and extraction of the plant samples

Sample leaves of *Strichnos spinosa* L were collected from Kumbotso Local Government, Kano State, Nigeria and identified at the Department of Plant Biology, Bayero University Kano with a herbarium accession number BUKHAN 0127 for reference.

The leaves were rinsed with distilled water, air dried under shade, ground to powder, sieved through a 75µm mesh and 500g of the powdered sample was soaked in 2 L of 95% ethanol solution for two weeks. The soaked samples were filtered using Whatmann No 1 filter paper. The filtrate sample was concentrated to thick syrup using a rotavapor (model: Recirculating chiller-F105), which was allowed to dry by expelling the excess ethanol. The dried extract obtained was used in preparing different concentrations of the inhibitor by dissolving 0.2, 0.4 and 0.6g of the extracts in 1 litre 0.9M HCl solution [13].

2.3 Weight loss Measurements

All the weighing of the Aluminium specimens, before and after immersion, was done using analytical weighing balance. A previously weighed metal (Aluminium) coupon was completely immersed in 100 ml of the various test solutions of 0.0, 0.2, 0.4 and 0.6g/L prepared in 0.9M HCl concentration in an open beaker. Each beaker was covered with polythene, banded with rubber band and inserted into a water bath maintained differently at various temperatures of 303, 313 and 323K. After every one hour the test sample was withdrawn from the test solution, washed with distilled water and then dipped in ethanol to dry. The washed coupon was rinsed in acetone and air dried before re-weighing. The total period of the experiment was four hours. From the change in the weights of the specimens, the corrosion rates (CR), the degree of surface coverage (θ) and inhibition efficiency (%I.E) of the inhibited and uninhibited samples were calculated using the following equations 1, 2 and 3 [14].

$$CR = \frac{\Delta W}{At} \quad (1)$$

$$\theta = \frac{\%\, I.E}{100} \quad (2)$$

$$\%\, I.E = \frac{W_f - W_i}{W_f} X\ 100 \quad (3)$$

Where W_f and W_i are the weight losses (g) for alumimium coupon in the absence and presence of the inhibitor respectively, θ is the degree of surface coverage of the inhibitor, $\Delta W = W_f - W_i$, A is the area of the Aluminium coupon (cm^2), t is the period of immersion (hours) and CR is the change in weight loss of Aluminium with time, t.

2.4 Fourier transform infrared (FT-IR) analysis

FTIR Instrument of model: Cary 630 FTIR Spectrophotometer (Agilent Technologies) was used to identify the major functional groups present in leaves extract of *Strichnos spinosa L.*, corroded Aluminium sample, and corrosion product of inhibited Aluminium metal in 0.9M HCl solution.

Each coupon was separately dipped in 100 mL of 0.9M HCl of acid-inhibitor concentration respectively for 4 hours to form an adsorbed layer after which they were removed, dried and scraped with a sharp razor blade taken for analysis. The analysis was done by scanning the sample through a wave number range of 650-4000 cm^{-1}[15].

2.5 Theoretical modeling and simulation

All theoretical calculations were performed using the density functional theory (DFT) electronic structure programs ($DMol^3$) and Forcite quench dynamics as contained in the Materials Studio 7.0 software (Accelrys, Inc.).

3. Results and Discussion

3.1 Weight loss measurements

In Table 1, surface coverage, inhibition efficiencies and corrosion rates of *Strichnos spinosa* L. obtained from weight loss method are presented. From the results obtained, it is evident that the surface coverage and inhibition efficiency increase with increase in concentration of the inhibitor but decrease with increasing temperature [4, 5]. This performance may be due to the

increase in the adsorption of *Strichnos spinosa* L extract at the metal/electrolyte boundary on increasing its concentration. This inference established that *Strichnos spinosa* L extract acts as an efficient corrosion inhibitor. Also it can be observed from table 1 corrosion rate increases with rise in temperature even with an increase in the concentration of the plant extract [6]. This clearly shows that the deleterious effect of temperature outweighs that of increase in the plant extract concentration.

Table 1. Surface coverage, inhibition efficiencies of *Strichnos spinosa* L and corrosion rate of Aluminium and in 0.9M HCl at different temperatures

Temperature (K)	System	Surface Coverage (θ)	Inhibition Efficiency (% IE)	Corrosion rate ($gh^{-1}cm^{-2}$) x 10^{-2}
	0.0g/L	-	-	9.66
	0.2g/L	0.83	83.00	8.55
303	0.4g/L	0.85	84.87	7.96
	0.6g/L	0.86	86.01	6.99
	0.0g/L	-	-	8.65
	0.2g/L	0.82	82.00	9.12
313	0.4g/L	0.83	82.99	8.50
	0.6g/L	0.85	85.27	7.75
	0.0g/L	-	-	1.09
	0.2g/L	0.79	79.16	9.74
323	0.4g/L	0.81	80.86	9.01
	0.6g/L	0.85	84.72	8.43

3.2 Fourier transform infrared spectroscopy (FTIR)

The functional groups present within the adsorption film that result during the adsorption process were investigated using FTIR technique. The FTIR spectra of the studied *Strichnos spinosa* L extract and Aluminium surfaces after corrosion in the presence of *Strichnos spinosa* L are shown in Figures 1.

IR spectra recorded for *Strichnos spinosa* L extract is depicted in Figure 1a. An absorption peak at 3301 cm^{-1} is assigned for linked -OH groups. The peaks at 2925 and 2854 cm^{-1} correspond to aliphatic stretching and alkane stretching of C–H groups. The peak at 2113 cm^{-1} correspond to alkyne stretching of C≡C, 1704, 1629 cm^{-1} are attributed to the stretching vibration of C=O groups. Peaks at 1514 cm^{-1} correspond to asymmetric stretching of N=O, 1443-1439 cm^{-1} are attributed to the alkane bending of C–H groups. The stretching mode of C–N group was confirmed by the peaks present at the wave numbers 1279, 1268 and 1171 cm^{-1}, all these were absent in figure 1b (which is the uninhibited corroded Al in 0.9M HCl). On the other hand in figure 1c, C–Cl stretch at 817 and 769 cm^{-1} were absent, suggesting that these bonds were used for the adsorption of the inhibitor onto the surface of the Aluminium.

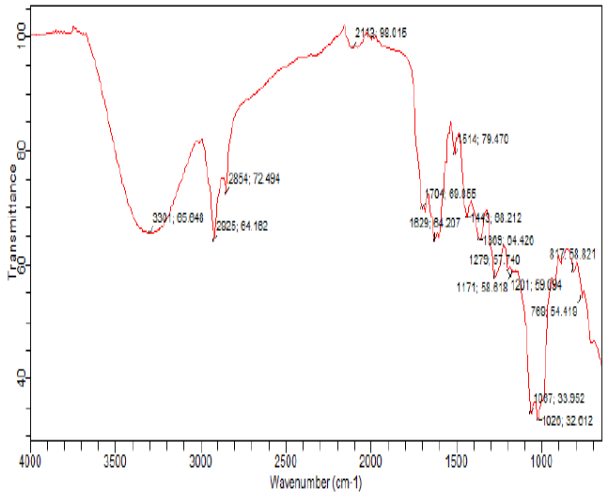

Fig 1. FTIR Spectrum of (a) leaves extract of *Strichnos spinosa* L, (b) corrosion product of Aluminium immersed in blank 0.9M HCl, (c) corrosion product of Aluminium immersed in inhibited 0.9M HCl

3.3 Adsorption isotherm studies

Adsorption isotherms were employed to describe the interaction between inhibitor and the surface of Al metal. In this study, results obtained for the degree of surface coverage (Θ) at all temperatures were fitted into different adsorption isotherms models. Figure 2 shows the Freundlich adsorption isotherm for *Strichnos spinosa L*. extract. From table 2, R^2values obtained of which is closer to unity, indicates a high degree of fitness adsorption data to the model. The tests revealed that the Freundlich adsorption model best described the adsorption characteristics of the studied plant extract. The values of K_{ads} obtained from the intercept were used to calculate the standard free energy (ΔG_{ads}) via using equation 4:

$\Delta G_{ads} = -RTIn(K_{ads}55.5)$ (4)

Where R is the molar gas constant, T is the absolute temperature and 55.5 is the concentration of water in solution expressed in M.

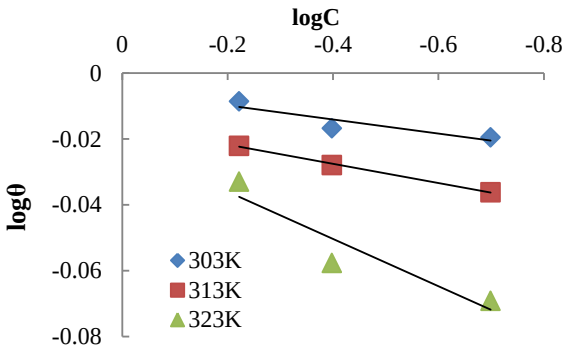

Fig 2. Freundlich isotherm for *Strichnos spinosa* L on Aluminium surface in 0.9M HCl solutions at various temperatures

Table 2. Adsorption isotherms for *Strichnos spinosa* L in 0.9 M HCl

Isotherms	Temp (K)	Slope	R^2	K_{ads}	ΔG x 10^3 ($Jmol^{-1}$)
Langmuir	303	0.388	0.587	0.205	-6127
	313	0.210	0.576	0.410	-8133
	323	0.111	0.585	0.605	-9438
Freundlich	303	0.032	0.999	0.875	-9769
	313	0.064	0.870	0.927	-10256
	323	0.058	0.874	0.867	-10584

From table 2, the calculated values of standard free energy of adsorption process were negative for all methods used and range from −6127 to −10584 $Jmol^{-1}$ for *Strichnos spinosa* L. The negative value of ΔG_{ads} indicates that the adsorption of inhibitor on the Aluminium surface substrates occurs spontaneously. Usually, values of standard free energy values lesser or closer to $-2000Jmol^{-1}$ are reliable with electric charges between molecules inhibitor and surface charged steel substrate (physisorption) while those more negative than $-40000Jmol^{-1}$ involves sharing of electrons from the inhibitor molecules to the metal surface to form a chemical bonding (chemisorptions) [16]. In the case of *Strichnos spinosa L*, ΔG_{ads} value of the inhibitor was found to be from −6127 to −10584 $Jmol^{-1}$, this indicates the phenomena of adsorption of inhibitor on the metal surface by physical adsorption process [10-12].

3.4 Effect of temperature

The effects of temperature on the corrosion rate and inhibition efficiency enable the calculation of kinetic and thermodynamic parameters for the inhibition and the adsorption processes. These parameters are useful in interpreting the nature/type of adsorption occurring between the inhibitor and the metal surface. The result reported in Table 1 shows that inhibition efficiency of *Strichnos spinosa L* decreased with increase in temperature. The value of activation energy (Ea) was calculated using the Arrhenius law equations 5 and 6 respectively [17]:

$$\frac{lnCR}{T} = lnA - Ea/RT \quad (5)$$

$$\frac{lnCR}{T} = ln(R/N_A h + \Delta S_a/RT) - \Delta Ha/RT \quad (6)$$

Where A is a constant which depends on the metal type, R is the universal gas constant, and T is the absolute temperature. The plot of ln(CR/T) versus reciprocal of absolute temperature (1/T) gave a straight line with slope = $-E_a/R$, from which the activation energy values for the corrosion process was calculated. The Arrhenius plot for the corrosion of Aluminium metal in 0.9MHCl acid in the absence and in the presence of different concentrations of inhibitor is shown in Figure 3.

The plot of ln(CR/T) versus reciprocal of absolute temperature (1/T) from equation 6, is as shown in Figure 4 gave a straight line with slope = $-\Delta H_a/R$, and intercept of $ln(R/N_A h + \Delta S_a/RT)$ from which the activation enthalpy energy and entropy values for the corrosion process was calculated. The values of E_a, ΔH_a and ΔS_a are represented in table 3.

The addition of inhibitor increased the energy of activation value (E_a). This change may be attributed to the change in the mechanism of the corrosion process through physical adsorption in the presence of inhibitor molecules [18]. The energy of activation (E_a) values in the presence of the *Strichnos spinosa* L increased drastically with the adsorption of components of *Strichnos spinosa* L on the Aluminium surface of the metal [18]. Negative values of entropies show that the activated complex in the rate determining step is an association rather than dissociation step meaning that a decrease in disordering takes place on going from reactants to the activated complex [19].

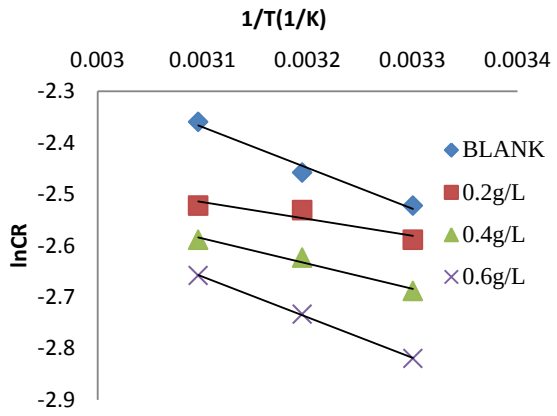

Figure 3: Arrhenius plots for the corrosion of Aluminium in 0.9 m hcl at different concentrations of *Strichnos spinosa* L.

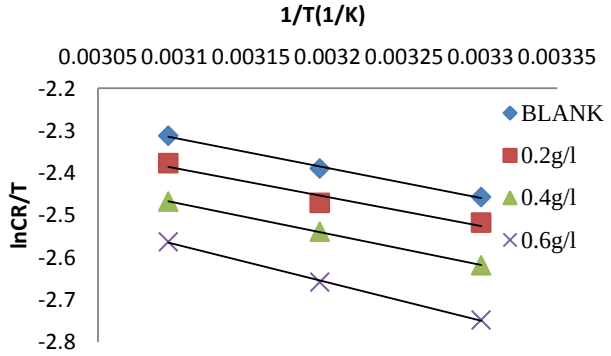

Fig 4. Variation of natural log (Corrosion Rate) of Aluminium with inverse temperature in 0.9 M HCl containing various concentration of *Strichnos spinosa L*.

Table 3. Thermodynamic parameters for dissolution of Aluminium metal in 0.9M HCl in different concentrations of *Strichnos spinosa* L.

Concentration (g/L)	E_a x 10^3 (J/mol)	ΔH_a x 10^3 (J/mol)	ΔS_a x 10^3 (J/mol)
Blank	43.38	44.87	-0.160
0.2	67.10	48.70	-0.168
0.4	68.07	44.92	-0.190
0.6	69.10	39.95	-0.164

3.5 Theoretical and Molecular dynamic Stimulation

The inhibiting action of *Strichnos spinosa* L extract, like other natural product extracts, can be attributed to the adsorption of the phytochemical constituents (flavonoids, triterpernoids, saponins, tannins, etc.) on the Aluminium metal surface. Accurate experimental determination of the contributions of the different constituents to the overall inhibiting effect is considerably hindered by the complex chemical compositions of its biomass extract. In the present work, the use of quantum chemical parameters and molecular dynamics simulations to highlight the individual contributions of some isolated compounds of *Strichnos spinosa* L extract obtained from literature [12] was evaluated. Such calculations were performed to describe the electronic structures of some of the major chemical constituents of the leaves of *Strichnos spinosa L*; Betulinic acid, Ursolic acid and Erythrodiol with a view to establishing the active sites as well as local reactivity of the molecules. The simulations were performed by means of the density functional theory (DFT) electronic structure program DMol^3 using a Mulliken population analysis [20]. Electronic parameters for the simulation included restricted spin polarization using the DND basis set and the Perdew–Wang (PW) local correlation density functional [5, 20]. Local reactivity of the studied compounds was analysed by means of the Fukui indices (FI) to assess regions of nucleophilic and electrophilic behaviour [21, 22]. Other parameters such as global hardness (η) and softness (σ) which are being calculated according to Koopman's theory, from the values of E_{HUMO} and E_{LUMO} using equation 12 and 13 [5], electronegativity (χ) and local softness s(r). Thus, for an N-electron system with total electronic energy E and an external potential v(r), the chemical potential μ, known as the negative of the electronegativity χ, has been defined as the first derivative of E with respect to N at constant v(r) as in equation 7:

$$\chi = -\mu = -\left(\frac{\partial E}{\partial N}\right) v(r) \qquad (7)$$

Hardness (η) has been defined within DFT as the second derivative of E with respect to N at constant v(r) as in equation 8 [2]:

$$\eta = \left(\frac{\partial^2 E}{\partial N^2}\right) v(r) = \left(\frac{\partial \mu}{\partial N}\right) v(r) \qquad (8)$$

The number of electrons transferred (ΔN) from the inhibitor molecule to the Aluminium metal surface was calculated by using equation 9:

$$\Delta N = \frac{(\chi_{Al} - \chi_{inh})}{2(\eta_{Al} - \eta_{inh})} \qquad (9)$$

where χ_{Al} and χ_{inh} denote the absolute electronegativity of Aluminium and the inhibitor molecule, respectively, and η_{Al} and η_{inh} denote the absolute hardness of Aluminium and the inhibitor molecule, respectively. Electron affinity (I) and ionization potential (A) are related in turn to the energy of the highest occupied molecular orbital (E_{HOMO}) and of the lowest unoccupied molecular orbital (E_{LUMO}) using the equations (10) and (11) [23]:

$$I = -E_{HOMO} \qquad (10)$$

$$A = -E_{LUMO} \qquad (11)$$

These quantities are related to the electron affinity (A) and ionization potential (I) using equations (10) and (11):

$$\chi = \left(\frac{I+A}{2}\right) = -\frac{E_{LUMO}+E_{HOMO}}{2} \quad (12)$$

$$\eta = \left(\frac{I-A}{2}\right) = -\frac{E_{LUMO}-E_{HOMO}}{2} \quad (13)$$

Global softness can also be defined in equation (14):

$$\sigma = \frac{1}{\eta} \quad (14)$$

The Fukui function f(r) is defined as the first derivative of the electronic density q(r) with respect to the number of electrons N at constant external potential v(r). Thus, using a scheme of finite difference approximations from Mulliken population analysis of atoms in the isolated compounds and depending on the direction of electron transfer, we have equations (15), (16), (17) [24]:

a. For nucleophilic attack

$$f_k^+ = q_k(N+1) - q_k(N) \quad (15)$$

b. For electrophilic attack

$$f_k^- = q_k(N) - q_k(N-1) \quad (16)$$

c. For radical attack

$$f_k^0 = \frac{q_k(N+1) - q_k(N-1)}{2} \quad (17)$$

Where q_k is the gross charge of atom k in the molecule, i.e., the electron density at a point r in space around the molecule. N corresponds to the number of electrons in the molecule. N + 1 corresponds to an anion, with an electron added to the LUMO of the neutral molecule; N - 1 corresponds to the cation with an electro. All calculations were done at the ground state geometry and electrons removed from the HOMO of the neutral molecule. These functions were condensed to the nuclei by using an atomic charge partitioning scheme, such as Mulliken population analysis in equations (15-17).

3.5.1 Quantum chemical calculations

Quantum chemical calculations provide crucial information regarding the reactivity and selectivity parameters of the inhibitor molecules [25]. Inhibitor molecules possess a variety of regions within themselves; this means that these regions have different tendencies of interactions with the surface of the metal. The reactivity and selectivity parameters can be utilized to determine and identify the molecular regions that have the tendency to react with the surface of the metal [26]. The reactivity of inhibitor compounds depends on the electronic properties such as electron density and partial charges on the atoms, among others. These electronic properties have their influence from the type and nature of the functional groups that are within the inhibitor molecules [20, 26]. Figures (5-7) below shows the optimized structure, total electron density, highest occupied molecular orbital (HOMO), lowest unoccupied molecular orbital (LUMO) of Betulinic acid, Ursolic acid and Erythrodiol compounds utilized in this study. The regions of high HOMO density are the sites at which electrophiles attack and represent the active centres, with the utmost ability to bond to the metal surface, whereas the LUMO orbital can accept the electrons in the p-orbital of the metal using antibonding orbitals to form feedback bonds from the Aluminium metal [27].

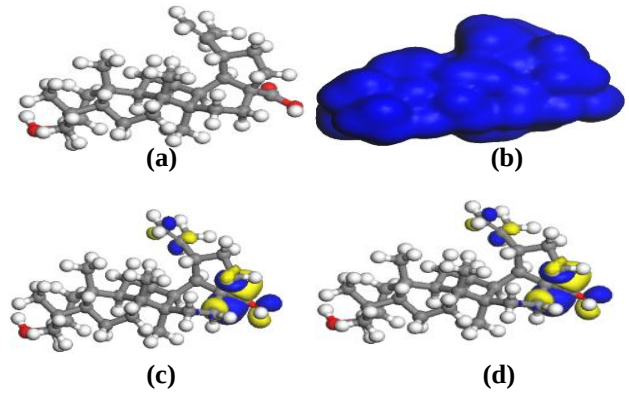

Fig 5. Electronic properties of Betulinic acid: (a) optimized structure, (b) total electron density (c) HOMO orbital, and (d) LUMO orbital (atom legend: *white* H, *light gray* C and *dark gray* O). The isosurfaces (larger lobes) depict the electron density difference; the *darker* regions show electron accumulation, whereas the *lighter* regions show electron loss

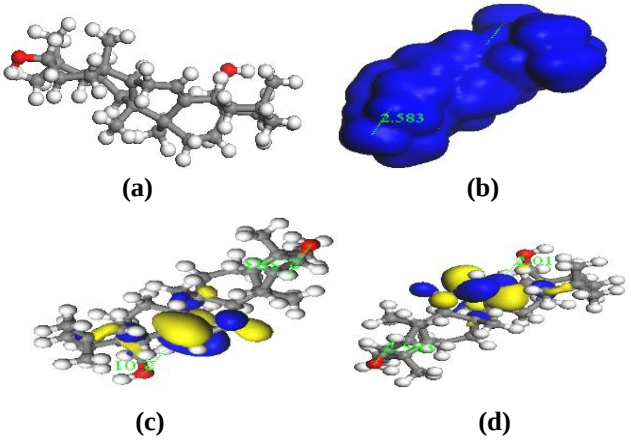

Fig 6. Electronic properties of Erythrodiol: (a) optimized structure, (b) total electron density (c) HOMO orbital, and (d) LUMO orbital (atom legend: *white* H, *light gray* C and *dark gray* O). The isosurfaces (larger lobes) depict the electron density difference; the *darker* regions show electron accumulation, whereas the *lighter* regions show electron loss

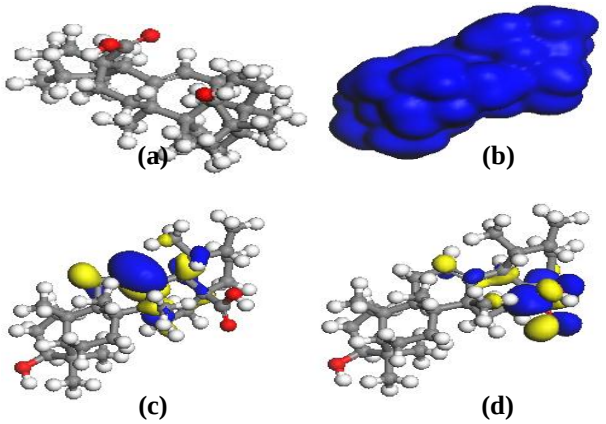

Fig 7. Electronic properties of Ursolic acid: (a) optimized structure, (b) total electron density (c) HOMO orbital, and (d) LUMO orbital (atom legend: *white* H, *light gray* C and *dark gray* O). The isosurfaces (larger lobes) depict the electron density difference; the *darker* regions show electron accumulation, whereas the *lighter* regions show electron loss.

Table 4. Computed Quantum Chemical Parameters (Electronic and Structural) of the Studied Inhibitor Molecules

Electronic/structural property	**Betulinic acid**	**Erythrodiol**	**Ursolic acid**
HOMO (orbital number)	252	246	208
LUMO (orbital number)	253	247	209
E_{HOMO} (eV)	-6.363	-5.624	-6.415
E_{LUMO} (eV)	-3.268	-3.417	-3.210
ΔE (eV)	3.095	2.207	3.205
Molecular Mass (g/mol)	457	443	457
Ionization Potential (eV)	6.363	5.624	6.415
Electron Affinity	3.268	3.417	3.210
Global Hardness (**η**)	1.548	1.104	1.603
Global Softness (**σ**)	0.646	0.906	0.624
Electronegativity (**χ**)	4.816	4.521	4.813
Fractions of Electrons Transferred (ΔN)	0.253	0.489	0.245

The values of molecular quantum chemical parameters such as E_{HOMO}, E_{LUMO}, the energy gap ($\Delta E = E_{HOMO} - E_{LUMO}$), ionization potential, electron affinity absolute (global) hardness, global softness, absolute electronegativities and fraction of electron transferred respectively were provided in Table 4.

Table 4 showed that the inhibitor compound possessing the highest E_{HOMO} value is Erythrodiol (-5.624eV) while that with the lowest is Ursolic acid (-6.415eV). The extent to which the molecule can accept electrons is indicated by E_{LUMO} values. Literature reveals that molecules that possess lower values of E_{LUMO} have a greater tendency to accept electrons from the species that are electron rich [28]. From table 4, it can be observed that Ursolic acid has the highest value of -3.210eV while Erythrodiol is the lowest at -3.417eV. Further details regarding the reactivity of these compounds towards the metal surfaces can be obtained through investigation of the energy gap ΔE. The energy gap of the molecule can be directly related to its stability and consequently its tendency to react. Higher values of energy gap are associated with high stability of the compound and therefore a low tendency to react while lower values are associated with low stability of the compound and therefore a high tendency to react with other chemical species [28]. From the three compounds studied as reported in Table 4, Ursolic acid and Erythrodiol have the highest and lowest values of 3.205eV and 2.207 4eV, respectively. Global hardness (η) of the inhibitor compounds provides more insight regarding the resistance of an atom to a charge transfer. This implies that compounds with high values of global hardness have a higher resistance of their atoms to charge transfers [5]. The inhibitor-metal adsorption process would be easier with the inhibitor compound that possesses lower values of global hardness. The other molecular property that compliments global hardness is known as global softness (σ). Together these molecular properties assist in the reactivity and selectivity of the inhibitor compounds. Global softness is related to the softness of the molecule as far the reactivity is concerned. The inhibitor-metal adsorption process could take place easily at the region of the inhibitor compound where global softness possesses the highest value [5]. From the results of this investigation, global hardness values are in such a way that Ursolic acid correspond to the highest value of 1.603 and Erythrodiol to the lowest value of 1.104 as reported in Table 4. The values of global softness are in such a way that Erythrodiol with the highest value of 0.906 while the lowest value of 0.624 is corresponding to Ursolic acid. One other imperative chemical reactivity parameter is the electronegativity (**χ**) of these compounds. This parameter gives information regarding the electron density within the molecule. In other words, electronegativity provides a measure of the power of an electron or a group of atoms to attract electrons towards itself [29]. This means that the atom with the highest electronegativity value possess the highest power to attract electrons or a group of atoms towards its direction. Table 4 indicates that Betulinic acid has the highest value of 4.816 eV while the lowest one is 4.521eV corresponding to Erythrodiol.

The ionization potential (I) is a molecular reactivity parameter which is very useful in the understanding of the reactivity and selectivity of inhibitor compounds. It gives information on the amount of energy that is required in order to remove an electron from a molecule [29]. In other words, the amount of energy that is released by a molecule during the inhibitor-metal adsorption process when an electron is lost can be predicted through an investigation of the ionization potential. From table 4, the fraction of

electron transferred was found to be highest in Erythrodiol than in others according to the trend: Erythrodiol > Betulinic acid > Ursolic acid. It was reported that if ΔN is less than 3.6, inhibition efficiency increases with increasing values of the electron donating ability of the molecules, while values of ΔN greater than 3.6 indicate a decrease in inhibition efficiency with increase in electron donating ability of the inhibitor. The earlier case is found to be applicable to all the studied molecules since their ΔN values are all less than 3.6 [23].

Table 5 shows the local reactivity of each molecule which was analyzed by means of the Fukui indices (FI) to assess reactive regions in terms of nucleophilic and electrophilic behavior. The f^- measures reactivity with respect to electrophilic attack, the propensity of the molecule to release electrons, whereas f^+ is a measure of reactivity relating to nucleophilic attack or tendency of the molecule attract electrons [25]. The obtained values for the studied molecules were presented in Table 5. The highest Mulliken and Hirshfeld charges at electrophilic (F^-) of the compounds are: Betulinic acid O (34,34), Erythrodiol O (32,33) and Ursolic acid C (3,3) While for the nucleophilic (F^+), Betulinic acid O (34,34), Erythrodiol C(27), O (32) and Ursolic acid O (3,3) respectively.

Table 5. Calculated Fukui Indices for the Studied Inhibitor Molecules

	Nucleophilic (f^+)		Electrophilic (f^-)	
Molecule	Mulliken	Hirshfield	Mulliken	Hirshfield
Betulinic	0(34)	O(34)	O(34)	O(34)
Acid	0.030	0.034	0.030	0.031
Erythrodiol	O(27)	O(32)	O(32)	O(33)
	0.014	0.025	0.012	0.025
Ursolic	O(3)	O(3)	O(3)	O(3)
Acid	0.097	0.098	0.097	0.097

3.5.2 Molecular dynamics (MD) simulation

Molecular dynamics (MD) simulation of the interaction between a single molecule and the Al surface was performed using Forcite quench MD in Material Studio (MS) Modelling 7.0 software to sample many different low-energy minima and to determine the global energy minimum [20]. Calculations were carried out in a 9 x 3 supercell using the condensed-phase optimized molecular potentials for atomistic simulation studies (COMPASS) force field and the Smart algorithm. Of the many kinds of Al surfaces, Al (1 1 0) is the most densely packed and also the most stable [30]. The Al crystal was cleaved along the (1 1 0) plane. The Al slab built for the simulation process was significantly larger than the inhibitor molecules in order to avoid edge effects during docking. Temperature was fixed at 350 K, with NVE (microcanonical) ensemble, with time step of 1 fs and simulation time of 5 ps. The system was quenched every 250 steps with the Al (1 1 0) surface atoms constrained. Optimized structure of the inhibitor molecule was used for the simulation. Adsorption of a single molecule of the phytochemical from *Strichnos spinosa L* extract sourced from literature onto the Al (1 1 0) surface provides access to the adsorption energetics and its effect on the inhibition efficiency of molecule. Thus, the adsorption energy, E_{ads}, between each phytochemical molecule of *Strichnos spinosa* L leaves extract obtained from literature compound molecule and Al (1 1 0) surface was calculated using equation 18 [30].

$$E_{\text{ads}} = E_{total} - (E_{mol} - E_{Al}) \qquad (18)$$

Where E_{mol}, E_{Al} and E_{total} correspond to the total energies of molecule, Al (1 1 0) slab and the adsorbed Mol/Al (1 1 0) couple in a gas phase.

Figure 8 (a-c) represents the snapshots of the side view of the lowest energy of the Molecular dynamics (MD) simulation of the interaction between a single molecule and the Al (1 1 0) surface which was performed using Forcite quench MD in Material Studio and of each of the *Strichnos spinosa L* extract obtained from literature compounds. The total energies were calculated by averaging the energies of the five (5) most stable representative adsorption configurations. From table 6, the obtained E_{ads} values; -57.318 kcal/mol for Betulinic acid, -45.693 kcal/mol for Erythrodiol and -63.435 kcal/ mol for Ursolic acid are all negative and of considerable magnitude, suggesting stable adsorption structures. The trend in E_{ads} corresponds to the trend in molecular size, showing that the larger molecules are more strongly adsorbed on the Al metal surface. It has also been reported that the more negative the adsorption energy of the inhibitor metal surface is, the better the adsorption of the inhibitor onto the metal surface and subsequently the higher the inhibition [5]. It can be observed from Table 6 that a trend could be inferred in terms of inhibition efficiencies of the inhibitors in respect of their adsorption energies as follows: Ursolic acid > Betulinic acid > Erythrodiol .

Table 6. Calculated Adsorption Parameters for the Interaction of the Studied Molecules with the Al(110) Surface Using Forcite Quench Dynamics

Parameters/ Molecules	Betulinic Acid	Erythrodiol	Ursolic Acid
Total Potential Energy (kcal/mol)	–-117.86	-40.86	–-342.46
Energy of Molecule (kcal/mol)	–-54.76	–-56.55	-71.49
Energy of Al (110) Surface (kcal/mol)	0.000	0.000	0.000
Adsorption Energy (kcal/mol)	–-57.32	–-45.69	-63.44

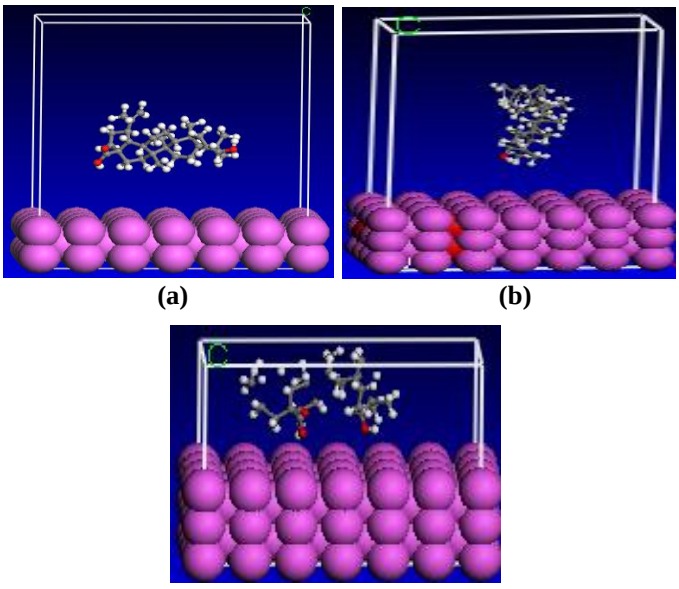

(a) **(b)**

(c)

Fig 8 (a-c). Adsorption of Single a) Betulinic acid b) Erythrodiol c) Ursolic acid Molecules on Aluminium (110) Surface

4. Conclusions

This study has revealed that extracts of *Strichnos spinosa L* effectively inhibit Aluminium metal corrosion in 0.9 M HCl. The result of Fourier transform infrared spectroscopy (FTIR) indicated that the corrosion reaction was inhibited by the adsorption of the phytochemicals onto the corroding Aluminium metal surface. The trends of inhibition efficiency with temperature as well as values of kinetic and activation parameters for corrosion and corrosion inhibition processes point toward significant physiosorption of the extract constituents on the Aluminium metal surface. Molecular dynamic quench stimulation was used to theoretically model the physiosorptive interactions between the plant extract's molecules, which are the active components of the extract and Al (1 1 0) surface. The magnitude of the obtained adsorption energy (ie less than -100kcal/mol) confirms strong physiosorption of the molecules onto the Al surface.

Acknowledgements

The authors wish to acknowledge the contributions of the Department of Pure and Industrial Chemistry, Bayero University Kano, Nigeria, for providing the chemical/reagents/instruments needed for this research and also appreciate the contribution of Dr. David Arthur of the Baze University, Abuja, Nigeria for the initial installation of the Accelrys Materials Studio 8.0 software programme.

Conflict of Interest

The authors declare that they have no conflict of interest.

References

1. Siaka AA, Eddy NO, Idris SO, Magaji L. Experimental and computational study of corrosion potentials of penicillin G. *Research Journal of Applied Sciences*. 2011;6(7-12):487-493.
2. Suedile F, Robert F, Roos C, Lebrini M. Corrosion inhibition of zinc by Mansoa alliacea plant extract in sodium chloride media: extraction, characterization and electrochemical studies. *Electrochimica Acta*. 2014;133:631-638.
3. Bammou L, Belkhaouda M, Salghi R, Benali O, Zarrouk A, Zarrok H, Hammouti B. Corrosion inhibition of steel in sulfuric acidic solution by the Chenopodium Ambrosioides Extracts. *Journal of the Association of Arab Universities for Basic and Applied Sciences*. 2014;16:83-90.
4. Dominic OO, Monday O. Optimization of the inhibition efficiency of Mango extract as corrosion inhibitor of mild steel in 1.0 M H_2SO_4 using response surface methodology. *Journal of Chemical Technology & Metallurgy*. 2016;51(3)302-314
5. Awe FE, Idris SO, Abdulwahab M, Oguzie EE. Theoretical and experimental inhibitive properties of mild steel in HCl by ethanolic extract of Boscia senegalensis. *Cogent Chemistry*. 2015;1(1):1-14.
6. Khadraoui A, Khelifa A, Hachama K, Mehdaoui R. Thymus Algeriensis extract as a new eco-friendly corrosion inhibitor for 2024 Aluminium alloy in 1 M HCl medium. *Journal of Molecular Liquids*. 2016;214:293-297.
7. Njoku DI, Onuoha GN, Oguzie EE, Oguzie KL, Egbedina AA, Alshawabkeh AN. Nicotiana tabacum leaf extract protects Aluminium alloy AA3003 from acid attack. *Arab.J.Chem*. https://doi.org/10.1016/j.arabjc.2016.07.017
8. Singh A, Ahamad I, Quraishi MA. Piper longum extract as green corrosion inhibitor for aluminium in NaOH solution. *Arabian Journal of Chemistry*. 2016;9:S1584- S1589.
9. Chaubey N, Savita, Singh VK, Quraishi MA. Corrosion inhibition performance of different bark extracts on aluminium in alkaline solution. *Journal of the Association of Arab Universities for Basic and Applied Sciences*. 2017;22(1):38-44.
10. Chaubey N, Yadav DK, Singh VK, Quraishi MA. A comparative study of leaves extracts for corrosion inhibition effect on aluminium alloy in alkaline medium. *Ain Shams Engineering Journal*. 2017;8(4):673-682.
11. Pramudita M, Sukirno S, Nasikin M. Synergistic Corrosion Inhibition Effect of Rice Husk Extract and KI for Mild Steel in H_2SO_4 Solution. *Bulletin of Chemical Reaction Engineering & Catalysis*. 2019;14(3):697-704.
12. Hoet S, Pieters L, Muccioli GG, Habib-Jiwan JL, Opperdoes FR, Quetin-Leclercq J. Antitrypanosomal activity of triterpenoids and sterols from the leaves of Strychnos spinosa and related compounds. *Journal of natural products*. 2007;70(8):1360-3.
13. Singh AK, Mohapatra S, Pani B. Corrosion inhibition effect of Aloe Vera gel: gravimetric and electrochemical study. *Journal of Industrial and Engineering Chemistry*. 2016;33:288-297.
14. Okafor PC, Ikpi ME, Ekanem UI, Ebenso EE. Effects of extracts from Nauclea latifolia on the dissolution of carbon steel in H2SO4 solutions. *Int. J. Electrochem. Sci*. 2013;8:12278-12286.

15. Sangeetha M, Rajendran S, Sathiyabama J, Krishnavenic A. Inhibition of corrosion of aluminium and its alloys by extracts of green inhibitors. *Portugaliae Electrochimica Acta*. 2013;31(1):41-52.
16. Singh A, Ebenso EE, Qurashi MA. Corrosion inhibition of carbon steel in HCl solution by some plant extracts. *International Journal of corrosion*. 2012;2012:1-20.
17. Meften MJ, Rajab NZ, Finjan MT. Synthesis of new heterocyclic compound used as corrosion inhibitor for crude oil pipelines. *American Scientific Research Journal for Engineering, Technology, and Sciences (ASRJETS)*. 2017;27(1):419-37.
18. Ouahrani MR, Gherraf N, lamine Sekirifa M, Baameur L. Anticorrosive Action Study of Retama Retam Extracts on Mild Steel X 52 in 20% H2SO4 Solution. *Energy Procedia*. 2014 Jan 1;50:401-405.
19. Xavier Stango SA, Vijayalakshmi U. Studies on corrosion inhibitory effect and adsorption behavior of waste materials on mild steel in acidic medium. *Journal of Asian Ceramic Societies*. ;6(1):20-29.
20. Ayuba AM., Uzairu A., Abba H, Shallangwa, GA.. Hydroxycarboxylic acids as corrosion inhibitors on Aluminium metal: a computational study, *Journal of Materials and Environmental Sciences*, 2018;9;11:3026-3034.
21. Eddy NO, Stoyanov SR, Ebenso EE. Fluoroquinolones as corrosion inhibitors for mild steel in acidic medium; experimental and theoretical studies. *Int. J. Electrochem. Sci.* 2010;5:1127-1150.
22. Eddy NO, Awe FE, Gimba CE, Ibisi NO, Ebenso EE. QSAR, Experimental and computational chemistry simulation studies on the inhibition potentials of some amino acids for the corrosion of mild steel in 0.1 M HCl. *Int. J. Electrochem. Sci*. 2011;6(4):931-957.
23. John S, Joseph A. Electro analytical, surface morphological and theoretical studies on the corrosion inhibition behavior of different 1, 2, 4-triazole precursors on mild steel in 1 M hydrochloric acid. *Materials Chemistry and Physics*. 2012;133(2-3):1083-1091.
24. Obot IB, Gasem ZM, Umoren SA. Understanding the mechanism of 2-mercaptobenzimidazole adsorption on Fe (110), Cu (111) and Al (111) surfaces: DFT and molecular dynamics simulations approaches. *Int. J. Electrochem. Sci*. 2014;9:2367-2378.
25. Udhayakala P, Samuel AM, Rajendiran TV, Gunasekaran S. DFT study on the adsorption mechanism of some phenyltetrazole substituted compounds as effective corrosion inhibitors for mild steel. *Der Pharma Chemica*. 2013;5(6):111-24.
26. Olasunkanmi LO, Obot IB, Kabanda MM, Ebenso EE. Some quinoxalin-6-yl derivatives as corrosion inhibitors for mild steel in hydrochloric acid: experimental and theoretical studies. *The Journal of Physical Chemistry C*. 2015;119(28):16004-16019.
27. Khaled KF, Abdel-Shafi NS, Al-Mobarak NA. Understanding corrosion inhibition of iron by 2-thiophenecarboxylic acid methyl ester: Electrochemical and computational study. *Int. J. Electrochem. Sci*. 2012;7:1027-1044.
28. Singh AK, Khan S, Singh A, Quraishi SM, Quraishi MA, Ebenso EE. Inhibitive effect of chloroquine towards corrosion of mild steel in hydrochloric acid solution. *Research on Chemical Intermediates*. 2013;39(3):1191-1208.
29. Martinez S. Inhibitory mechanism of mimosa tannin using molecular modeling and substitutional adsorption isotherms. *Materials Chemistry and Physics*. 2003;77(1):97-102.
30. Lgaz H, Salghi R, Chaouiki A, Jodeh S, Bhat KS. Pyrazoline derivatives as possible corrosion inhibitors for mild steel in acidic media: A combined experimental and theoretical approach. *Cogent Engineering*. 2018;5(1):1441585.

Recommended Citation

Ayuba AM, Ameenullah A. Corrosion inhibition potentials of *Strichnos spinosa* L. on Aluminium in 0.9M HCl medium: experimental and theoretical investigation, *Alg. J. Eng. Tech.* 2020; 3: 028-037. http://dx.doi.org/10.5281/zenodo.4402204